Available online at www.sciencedirect.com

SciVerse ScienceDirect

Geochimica et Cosmochimica Acta 111 (2013) 128–139

Geochimica et Cosmochimica Acta

www.elsevier.com/locate/gca

What does leaf wax δD from a mixed C_3/C_4 vegetation region tell us?

Yiming V. Wang [a,b,*], Thomas Larsen [b,c], Guillaume Leduc [a], Nils Andersen [b], Thomas Blanz [a], Ralph R. Schneider [a,b]

[a] Institute of Geosciences, Christian-Albrechts University of Kiel, Ludewig-Meyn-Str. 10-14, 24118 Kiel, Germany

[b] Leibniz-Laboratory for Radiometric Dating and Stable Isotope Research, Christian-Albrechts University of Kiel, Max-Eyth-Str. 11-13, 24118 Kiel, Germany

[c] Biogeodynamics and Biodiversity Group, Centre for Advanced Studies of Blanes (CEAB), Spanish Research Council (CSIC), 17300 Blanes, Catalonia, Spain

Available online 17 October 2012

Abstract

Hydrogen isotope values (δD) of sedimentary terrestrial leaf wax such as *n*-alkanes or *n*-acids have been used to map and understand past changes in rainfall amount in the tropics because δD of precipitation is commonly assumed as the first order controlling factor of leaf wax δD. Plant functional types and their photosynthetic pathways can also affect leaf wax δD but these biological effects are rarely taken into account in paleo studies relying on this rainfall proxy. To investigate how biological effects may influence δD values we here present a 37,000-year old record of δD and stable carbon isotopes ($\delta^{13}C$) measured on four *n*-alkanes (*n*-C_{27}, *n*-C_{29}, *n*-C_{31}, *n*-C_{33}) from a marine sediment core collected off the Zambezi River mouth. Our paleo $\delta^{13}C$ records suggest that each individual *n*-alkanes had different C_3/C_4 proportional contributions. *n*-C_{29} was mostly derived from a C_3 dicots (trees, shrubs and forbs) dominant vegetation throughout the entire record. In contrast, the longer chain *n*-C_{33} and *n*-C_{31} were mostly contributed by C_4 grasses during the Glacial period but shifted to a mixture of C_4 grasses and C_3 dicots during the Holocene. Strong correlations between δD and $\delta^{13}C$ values of *n*-C_{33} (correlation coefficient $R^2 = 0.75$, $n = 58$) and *n*-C_{31} ($R^2 = 0.48$, $n = 58$) suggest that their δD values were strongly influenced by changes in the relative contributions of C_3/C_4 plant types in contrast to *n*-C_{29} ($R^2 = 0.07$, $n = 58$). Within regions with variable C_3/C_4 input, we conclude that δD values of *n*-C_{29} are the most reliable and unbiased indicator for past changes in rainfall, and that δD and $\delta^{13}C$ values of *n*-C_{31} and *n*-C_{33} are sensitive to C_3/C_4 vegetation changes. Our results demonstrate that a robust interpretation of palaeohydrological data using *n*-alkane δD requires additional knowledge of regional vegetation changes from which *n*-alkanes are synthesized, and that the combination of δD and $\delta^{13}C$ values of multiple *n*-alkanes can help to differentiate biological effects from those related to the hydrological cycle.

1. INTRODUCTION

The stable hydrogen isotopic composition (δD) of long chain plant leaf wax derived from terrestrial plants (*n*-alkanes and *n*-acids) preserved in lake and marine sediments is one of the most promising tools for inferring changes in paleoprecipitation (e.g. Liu and Huang, 2005; Niedermeyer et al., 2010; Schefuss et al., 2005, 2011; Tierney et al., 2008). This new tool is largely based on studies comparing modern plant wax δD values with local precipitation and/or lake water δD values. These studies suggest that regional meteoric water δD values are the primary controls on the leaf wax signatures (Bi et al., 2005; Garcin et al., 2012; Hou et al., 2008; Polissar and Freeman, 2010; Feakins and Sessions, 2010; Sachse et al., 2004, 2006). Besides δD of mete-

* Corresponding author at: Institute of Geosciences, Christian-Albrechts University of Kiel, Ludewig-Meyn-Str. 10-14, 24118 Kiel, Germany. Tel.: +49 (431)8802861; fax: +49 (431)8801912.

E-mail address: ywang@leibniz.uni-kiel.de (Y.V. Wang).

0016-7037/$ - see front matter © 2012 Elsevier Ltd. All rights reserved.
http://dx.doi.org/10.1016/j.gca.2012.10.016

oric water, biological factors such as plant functional types and their photosynthetic pathways also affect the δD values of leaf wax (Bi et al., 2005; Chikaraishi and Naraoka, 2003; Garcin et al., 2012; Hou et al., 2007; Liu and Yang, 2008; Liu et al., 2006; McInerney et al., 2011; Pedentchouk et al., 2008; Smith and Freeman, 2006). It has been demonstrated that the significant differences in net apparent fractionation $\varepsilon_{lipid\text{-}w}$ from source water to lipids is associated with plant biosynthetic pathways (see Sachse et al., 2012 for a review). These differences in $\varepsilon_{lipid\text{-}w}$ are likely due to factors such as evapotranspiration processes and the location and timing of wax synthesis. Since these factors are particular for different plant functional types it can lead to large variations in $\varepsilon_{lipid\text{-}w}$ that are diagnostic of their biosynthetic origins such as C_4 and C_3 plants (i.e. Smith and Freeman, 2006; McInerney et al., 2011; Sachse et al., 2012). However, accounting for these biological factors has been particularly challenging in paleo δD records due to the difficulties in assessing the relative importance of environmental and biological factors controlling leaf wax δD values.

Owing to the isotopic difference resulting from physiological differences during CO_2 acquisition for photosynthesis (Cerling et al., 1997), carbon-isotopic composition ($\delta^{13}C$) signatures can serve as tracers for C_4 (using C_4 carbon metabolic pathway) and C_3 (using C_3 carbon metabolic pathway) plants, and therefore have been used as a proxy for determining the changes in composition and origin of continental vegetation (i.e. Huang et al., 2000, 2001). Parallel $\delta^{13}C$ measurements on long chain leaf wax in the same sedimentary sequence have been suggested as a potential tool for differentiating the influences of metabolic and/or plant functional types from that of precipitation (Garcin et al., 2012). A handful of studies have demonstrated that δD and $\delta^{13}C$ can be used to infer past changes in the hydrological cycle and in vegetation at low latitudes, respectively (see e.g. Schefuss et al., 2005; Niedemeyer et al., 2010; Tierney et al., 2008, 2010). A prerequisite for interpreting leaf wax δD as an indicator of changes in precipitation is to assume that vegetation remained relatively stable with a small range of $\delta^{13}C$ values throughout the studied time window (Schefuss et al., 2005; Niedemeyer et al., 2010). However, in areas with large shifts in C_3/C_4 plant types due to change in regional climate and/or in catchment area of a large river system it is essential to disentangle effects of precipitation from plant functional types on leaf wax δD values for a more reliable interpretation of leaf wax δD (Smith and Freeman, 2006; Garcin et al., 2012).

Additionally, leaf wax δD and $\delta^{13}C$ are often measured on the single most abundant leaf wax homologue (such as individual *n*-C_{29} and *n*-C_{31} alkanes or *n*-C_{28} acid), assuming that the most dominant individual leaf wax biomarker at catchment-scale reliably reflect the climatic conditions of the region (Collins et al., 2011; Konecky et al., 2011; Niedermeyer et al., 2010; Schefuss et al., 2005; Tierney et al., 2008, 2010). A number of observations from modern plants suggest the most abundant long chain *n*-alkanes (such as *n*-C_{27}, *n*-C_{29}, and *n*-C_{31}) from the same plant functional group respond similarly to climatic and environmental factors (Sessions et al., 1999; Chikaraishi and Naraoka, 2003; Yang and Huang, 2003; Bi et al., 2005; Liu et al., 2006; Sessions, 2006; Liu and Yang, 2008). However, in areas where the different plant functional types are changing, δD can reflect changes in rainfall as well as vegetation (Smith and Freeman, 2006; Liu and Yang, 2008). This is because the vegetation sources to individual *n*-alkanes or *n*-acid homologues can change during the studied time window and these vegetation sources may have different dominance of individual homologues. For example, previous studies show that C_4 grasses in southern African savannah are dominated by *n*-C_{31} and *n*-C_{33} homologues, whereas C_3 trees in woodland savannah are dominated by *n*-C_{29} and *n*-C_{31} homologues (Rommerskirchen et al., 2006; Vogts et al., 2009). Changes in plant functional types driven by changes in climate will eventually affect the δD values measured on individual homologues. As a result, the temporal changes in precipitation pattern deduced from leaf wax δD obtained in sedimentary sequences may vary depending upon which homologue was used to derive past changes in the hydrological cycle (e.g. Schefuss et al., 2011).

We present a new paleo-record of *n*-alkanes from a high-resolution marine sediment core retrieved in the Mozambique Channel close to the Zambezi River mouth. We examined the relative importance of changes in precipitation regimes and shifts in C_3/C_4 plant types on δD values of *n*-alkanes (δD_{alk}) by performing dual measurements of δD and $\delta^{13}C$ on four *n*-alkane homologues. Since the Zambezi River catchment area is composed of a mixed vegetation of C_3 woodland and C_4 grasses savannah (Still et al., 2003; Timberlake, 2000), we expect that the composition of C_3/C_4 plant functional types strongly influence our paleo δD records in addition to the influences from rainfall changes.

2. REGIONAL SETTING AND CLIMATE

We analyzed a marine sediment core (GIK 16160-3, 18°14.47′S, 37°52.11′E, 1339 m water depth) retrieved close to the Zambezi River mouth in the southwestern tropical Indian Ocean (Fig. 1). The Zambezi River rises in northwestern Zambia on the Central African Plateau. It is the largest river in southern Africa, and its catchment area (1.4×10^6 km^2, ~9–20°S and ~18–37°E) integrates substantial tropical southern African hydrological regions (Walford et al., 2005). Its runoff discharges an average of 82 km^3 per year into the Indian Ocean, so that marine sediments situated close to the river mouth provide excellent climate archives for recording continental climate changes (Schefuss et al., 2011). The rainfall seasonality in the Zambezi River catchment is connected to large-scale atmospheric patterns driven by changes in monsoonal flow originating in the tropical Indian Ocean as well as the seasonal migration of the Intertropcial convergence Zone (Goddard and Graham, 1999; Nicholson, 2000). Precipitation amounts are marked by a dry season occurring during austral winter in the catchment (Timberlake, 2000). The hydrology of the Zambezi River catchment is not uniform with generally high rainfall (1300 mm/yr) in the north and lower rainfall (600 mm/yr) in the south (Moore et al., 2007). The rainy season within the catchment area occurs when northeasterly winds transport moisture from the trop-

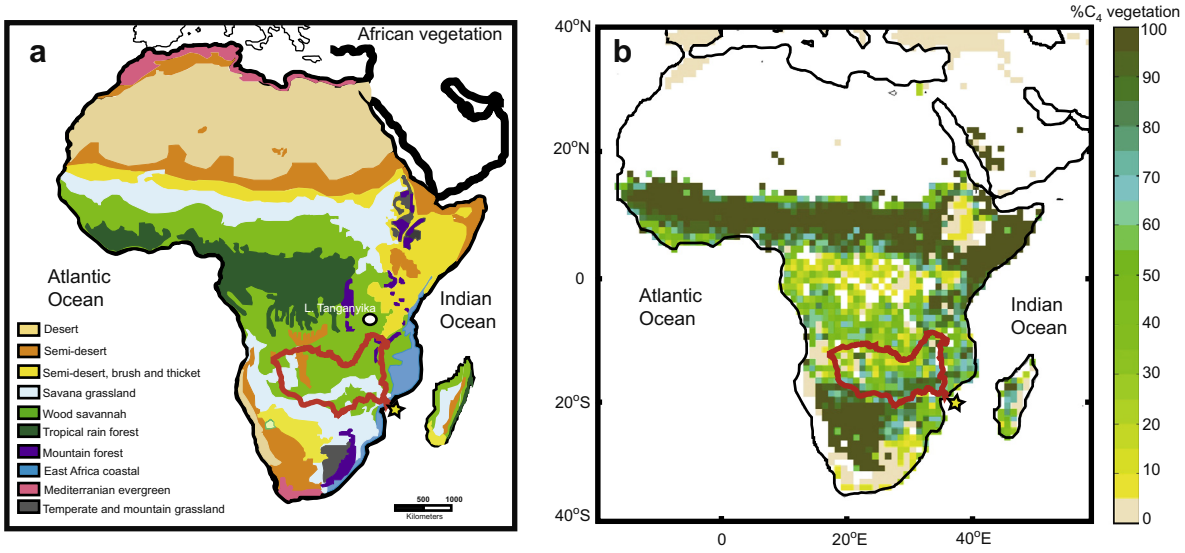

Fig. 1. Distribution of (a) modern vegetation types and (b) C_4 vs. C_3 plant vegetation distribution in Africa. The catchment area (red line) of the Zambezi River is composed of substantial mixtures of C_4 grassland and C_3 woodland savannah (redrawn from Still et al., 2003). GIK 16160-3 core location (yellow star) and Lake Tanganyika core site (white dot) were also indicated.

ical Indian Ocean to the tropical southern Africa during late spring to early autumn (Gimeno et al., 2010).

Vegetation in the Zambezi River catchment is very diverse (Timberlake, 2000). The Zambezian biome covers 95% of the basin, which is composed of a mixture of Panicoideae (mainly C_4) and Chloridoideae (C_4) grassland savannah and C_3 woodland savannah (Fig. 1), interspersed with lakes and wetlands where drainage is poor (Rommerskirchen et al., 2006; Timberlake, 2000). C_3 grasses are unlikely to play an important role in the tropical Africa (Still et al., 2003) and field survey shows that only 10% of grass species below ~2000 m elevations are C_3 grasses (Livingstone and Clayton, 1980).

3. THEORETICAL BACKGROUND FOR δD OF C4 GRASSES AND C3 DICOTYLEDONS (DICOTS)

Numerous studies have identified plant physiological factors affecting leaf wax δD values in addition to the source water isotopic composition (i.e. Liu and Yang, 2008; Smith and Freeman, 2006; McInerney et al., 2011). A recent literature review shows that the apparent fractionation factors ($\varepsilon_{alk\text{-}MAP}$) for three common *n*-alkanes (*n*-C_{27}, *n*-C_{29}, *n*-C_{31}) are highly coherent within the same plant functional group (Sachse et al., 2012). However $\varepsilon_{alk\text{-}MAP}$ are significantly different among plants using different photosynthetic pathways and plant functional types, for example C_3 and C_4 grasses, and C_3 trees, forbs and shrubs (Sachse et al., 2012).

Since *n*-C_{33} is also a dominant *n*-alkane for C_4 grasses in tropical Africa we synthesized from the literature $\varepsilon_{alk\text{-}MAP}$ values of four *n*-alkanes (*n*-C_{27}, *n*-C_{29}, *n*-C_{31}, *n*-C_{33}) for C_4 grasses and C_3 dicots, the dominant two vegetation types in our study area (see Supplementary data Appendix). We grouped C_3 dicot together including all trees, forbs and shrubs because we are not able to distinguish these functional groups from the sedimentary record. We calculated $\varepsilon_{alk\text{-}MAP}$ between *n*-alkanes and growth water following the formula $\varepsilon_{alk\text{-}MAP} = 1000[(\delta_{alk} + 1000)/(\delta_{MAP} + 1000) - 1]$ (Sessions et al., 1999) to account for variations in δD values caused by variables other than growth water. The measured δD values of growth water were used when available, otherwise the δD of local mean-annual precipitation (MAP) are assumed as δD of the growth water. The estimates of mean annual precipitation were performed using the Online Isotopes in Precipitation Calculator for each study location (Bowen, 2010; Bowen et al., 2009; Bowen and Revenaugh, 2003). The results are summarized in Fig. 2, and the statistics are presented in Table 1. We used R 2.12.1 (R-Development-Core-Team, 2010) to perform all statistical analyses.

We found that the four *n*-alkanes are highly coherent within the group of C_4 grasses or C_3 dicots (Table 1) similar to the observations by Sachse et al. (2012) for three homologues, further confirming that δD of one homologue *n*-alkane can be used to derive paleohydrological changes if the plant functional groups have not changed over time (i.e. Smith and Freeman, 2006; Liu and Yang, 2008; McInerney et al., 2011). Moreover, the $\varepsilon_{alk\text{-}MAP}$ of C_3 dicots (composed of shrubs, forbs and trees) is significantly more enriched by ~30‰ than that of C_4 grasses (Fig. 2, student-*t* test $p < 0.001$). The $\varepsilon_{alk\text{-}MAP}$ differences between C_3 woody plants and C_4 grasses may be explained by differences in leaf architecture as well as in location and timing of wax synthesis (Sachse et al., 2012). This result supports that the plant functional types in combination with their photosynthetic pathways can have an important effect on δD_{alk} (i.e. Smith and Freeman, 2006; McInerney et al., 2011). Therefore, the effect on δD from plant types need to be taken into account while interpreting the δD_{alk} in Zambezi

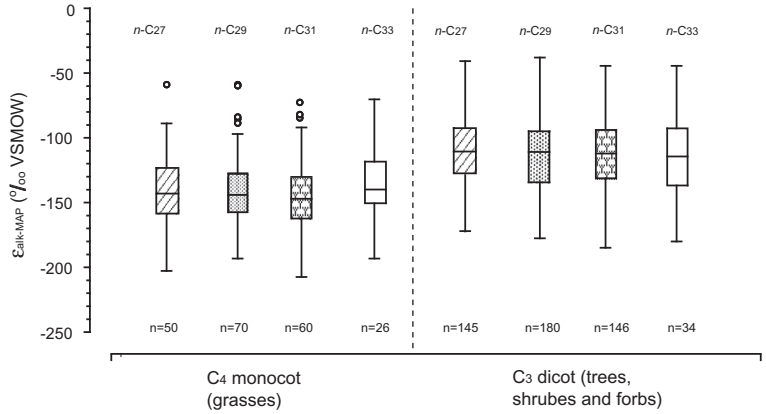

Fig. 2. Box plot of apparent fractionation ($\varepsilon_{alk\text{-}MAP}$) between the most common long chain n-alkanes (*n*-C_{27}, *n*-C_{29}, *n*-C_{31}, and *n*-C_{33}) and mean annual precipitation (MAP) categorized by photosynthetic pathway as well as plant function types: C_3 dicots and C_4 grasses. Student-t test shows that $\varepsilon_{alk\text{-}Map}$ across all four homologues of these two groups are significantly different ($p < 0.001$). The box plots show median (horizontal lines), upper and lower quartiles (boxes), and maximum and minimum values (vertical lines) in addition to any outliers, i.e. values that exceed the fifth or ninety-fifth percentile (open circles). Sample size (n) is indicated for each group. The values for δD of these long chain *n*-alkanes are taken from Bi et al. (2005), Chikaraishi and Naraoka (2003), Feakins and Sessions (2010), Hou et al. (2007), Krull et al. (2006), Liu et al., (2006), Liu and Yang (2008), Pedentchouk et al., (2008), Sachse et al., (2006, 2009), Smith and Freeman (2006), Yang and Huang (2003), and McInerney et al. (2011). The δD of MAP estimates of mean annual precipitation using the Online Isotopes in Precipitation Calculator (http://wateriso.eas.purdue.edu/waterisotopes/pages/data_access/oipc.html) based on Bowen and Revenaugh (2003), Bowen et al. (2009) and Bowen (2010) from sample locations.

Table 1
One-way ANOVA tests of differences in $\varepsilon_{alk\text{-}MAP}$ values between individual *n*-alkanes (*n*-C_{27}, *n*-C_{29}, *n*-C_{31} and *n*-C_{33}) within a plant functional type showing that the four homologues were not significantly different within each group. "SS" is sum of squares, "df" degrees of freedom and "F" the F ratio, "*p*" the *p*-value. For statistical purposes only samples with values of *all* four *n*-alkanes were included in this analysis.

Plant functional type	Dependent variable	Factors	SS	df	*F*	*p*
C_4 monocot	$\varepsilon_{l\text{-}MAP}$ values of ind. *n*-alkanes	*n*-C_{27}, *n*-C_{29}, *n*-C_{31}, *n*-C_{33}	1274	3	0.8354	0.479
		Residuals	38629	76		
C_3 dicot	$\varepsilon_{l\text{-}MAP}$ values of ind. *n*-alkanes	*n*-C_{27}, *n*-C_{29}, *n*-C_{31}, *n*-C_{33}	1136	3	0.300	0.826
		Residuals	126395	100		

River catchment, where the vegetation type is mainly composed of a mixture of C_3 woodland and C_4 grassland savannah (Fig. 1).

4. MATERIALS AND METHODS

4.1. Age control

The age model for core GIK 16160-3 is based on fifteen ^{14}C-AMS dates measured on mixed planktonic foraminifera fractions containing *Globigerinoides ruber*, *Globigerinoides trilobus* and *Globigerinoides sacculifer* at the Leibniz Laboratory for Radiometric Dating and Stable Isotope Research, University of Kiel (CAU) (Fig. 3). When *G. ruber* could provide sufficient sample mass, we used only *G. ruber* for radiocarbon dating (Table 2). We converted ^{14}C ages into calendar ages using CALIB 6 program (Stuiver and Reimer, 1993) with the Marine09 calibration curve (Reimer et al., 2009). We have taken the mean Delta R and Delta R error (191 ± 54 years) from two sites with known reservoir ages closest to our core location, Comoros and Mayotte (marine Reservoir correction database) (http://calib.qub.ac.uk/marine/) to correct for the constant reservoir age of 405 years embedded in the Marine09 calibration curve. We then performed a linear interpolation between adjacent radiocarbon dates. The 15 AMS dating results reveal a continuous sedimentation sequence and the GIK 16160-3 over the last 37,000 years (Table 2). A substantial increase in sedimentation rates from ~19 to 12 ka compared to the Glacial and Holocene time interval is probably linked to changes in sediment input from the nearby margin related to sea level rise that occurred during the Termination 1.

4.2. *n*-Alkane extractions and analyses

Approximately 8 g of homogenized dry sediment were extracted for total lipids with a mixture of dichloromethane and methanol (DCM:MeOH, 9:1 v:v) at 100 °C and at 100 bar for three 15 min cycles in a Accelerated Solvent Extractor (ASE200, Dionex Cooperation). Elemental sulfur was removed by stirring for 30 minutes with activated copper beads in DCM under vacuum. Lipids were partitioned into different fractions using column chromatography with activated silica gel (4 h at 450 °C). The saturated hydrocarbon fraction containing the *n*-alkanes was obtained by column chromatography over $AgNO_3$-impregnated silica eluted with hexane.

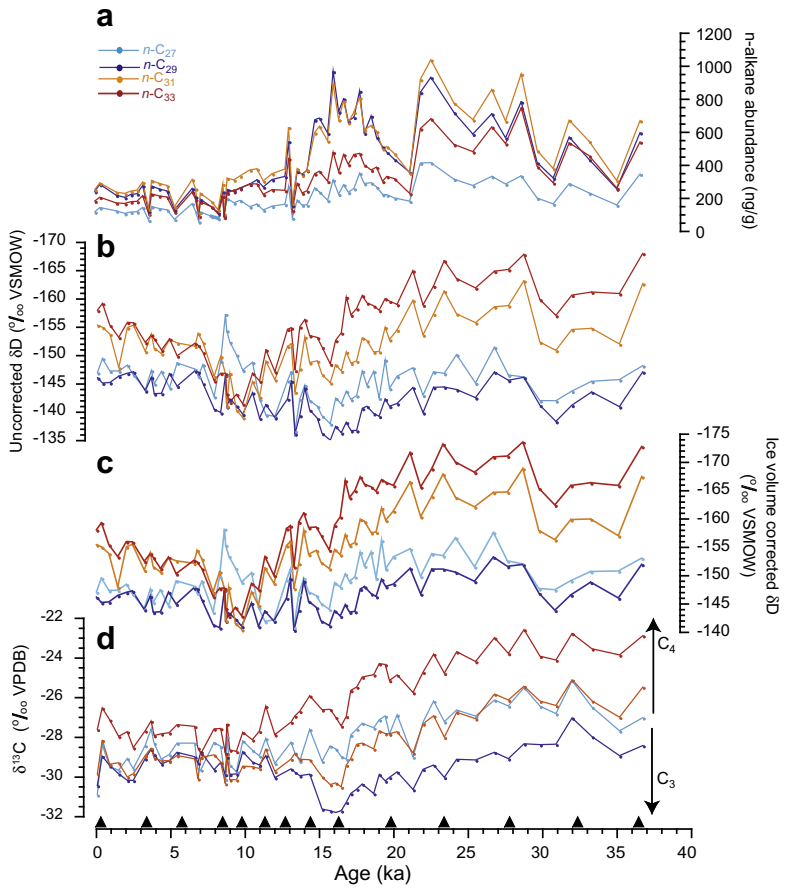

Fig. 3. (a) *n*-Alkane abundance; (b) uncorrected δD; (c) ice volume corrected δD for four *n*-alkanes (n-$C_{33,31,29,27}$) from core GIK16160-3. (d) $\delta^{13}C$ record for individual *n*-alkanes. Fifteen calibrated ^{14}C dates (filled triangle) based on planktonic foraminifera were also plotted. The more enriched $\delta^{13}C$ values indicates more C_4 vegetation contribution and the more depleted $\delta^{13}C$ indicates more C_3 vegetation type contribution.

Quantification and identification of compounds were performed with an Agilent 6890 N Gas Chromatograph (GC) with a Flame Ionization Detector, based on comparisons with a laboratory internal standard (a series of *n*-alkane mixtures). The saturated hydrocarbon fraction was analyzed in replicates for stable carbon ($\delta^{13}C$, $n = 3$ for each sample) and hydrogen (δD, $n = 7$–8 for each sample) isotopic compositions on a Thermo Finnigan MAT 253 mass spectrometer interfaced with a Thermo Finnigan GC combustion III (for $\delta^{13}C$) or High Temperature Conversion systems (for δD) at the Leibniz Laboratory, CAU. Individual *n*-alkanes were separated using an Agilent HP-5 capillary column (30 m × 0.32 mm × 0.25 μm). $\delta^{13}C$ is expressed relative to the VPDB scale, established by using Arndt Schimmelmann's stable isotope A2 reference mixture from 2009. The accuracy and precision of the system were determined daily by measuring an in-house mixture of n-C_{20} to n-C_{40} alkanes in between samples. The standard error of mean (S.E.) of $\delta^{13}C$ on internal standard was $\leqslant 0.2‰$ ($n = 2$ or 3 per sample). The S.E. for $\delta^{13}C$ of n-C_{27}, n-C_{29}, n-C_{31}, and n-C_{33} based on three measurements for sample were $\leqslant 0.22‰$. Due to small error ranges for all samples, error bars on each sample were not plotted.

Pyrolytic conversion of organic hydrogen to H_2 was conducted at 1450 °C. Measurements of the H_3^+ factor were determined daily using H_2 reference gas. The H_3^+ factor varied between 6.95 and 7.55 ppm nA^{-1} over a period of 5 months, averaging 7.15 ppm nA^{-1}, with a standard deviation of 0.13 ppm nA^{-1}. δD values of our in-house mixture of n-C_{20} to n-C_{40} alkanes were calculated relative to pulses of reference H_2 gas and were calibrated against the VSMOW scale by reference to H_2 produced from co-injected A2 mixture (available from A. Schimmelmann, Biogeochemical Laboratories, Indiana University). Data were then normalized to the VSMOW isotopic scale by using linear regression to our in-house *n*-alkane mixture, which is running daily with samples. S.E. for δD of the in-house standard (average $n = 8$ per day) was 0.7‰ or better for all compounds. The S.E. for δD of n-C_{27}, n-C_{29}, n-C_{31}, and n-C_{33} based on 7 or 8 measurements for each sample were $\leqslant 0.87‰$. Similar to $\delta^{13}C$, we did not plot the error bar because of such small error ranges for all samples.

4.3. CPI and ACL

We calculated the Carbon Preference Index (CPI) and Average Chain Length (ACL). The CPI is used to examine

Table 2
^{14}C-AMS dates used for the chronology of GIK 16160-3.

Sample	Core depth (cm)	Foraminferal taxa used for dating	^{14}C age (^{14}C yr BP)	Error (^{14}C yr)	Calendar age range (1σ) (yr BP)	Calendar age (ka)[†]
KIA 41415	18	*G. ruber* + *G. trilobus* + *G. sacculifer*	1225	25	554–650	605
KIA 43167	96.5	*G. ruber*	3970	30	3638–3809	3721
KIA 41416	163	*G. ruber*	5835	35	5965–6135	6049
KIA 41417	223	*G. ruber*	8305	45	8539–8758	8659
KIA 41418	253	*G. ruber*	9930	50	9793–10078	9914
KIA 41419	287	*G. ruber*	10560	60	11235–11618	11432
KIA 41420	313	*G. ruber* + *G.trilobus* + *G. sacculifer*	11620	70	12781–12984	12906
KIA 41421	363.5	*G. ruber*	13070	70	14465–14883	14595
KIA 41422	392.5	*G. ruber* + *G.trilobus* + *G. sacculifer*	13590	70	15204–15904	15641
KIA 43168	426	*G. ruber* + *G.trilobus*	14270	70	16716–16914	16812
KIA 41424	527.5	*G. ruber*	17170	120	19826–20137	19923
KIA 41425	582.5	*G. ruber*	20560	160	23608–24125	23850
KIA 43169	625	*G. ruber*	23750	190	27764–28267	28005
KIA 41426	667.5	*G. ruber*	28990	430	31937–33155	32581
KIA 43179	691	*G. ruber*	32750	590	35589–37511	36728

[†] Median age.

the odd over even carbon number predominance to distinguish terrestrial plant from petroleum sources (Marzi et al., 1993). ACL is to assess the dominace of the *n*-alkanes. The CPI is defined as:

$$\mathrm{CPI} = \frac{\sum(X_i + X_{i+1} + \ldots + X_n) + \sum(X_{i+2} + \ldots + X_{n+2})}{2 \times \sum(X_{i+1} + \ldots + X_{n+1})} \quad (1)$$

$i = 25$, $n = 33$. X_i refers to the abundance of the *n*-alkane with number of carbon atoms.

The ACL is defined as:

$$\mathrm{The\ ACL} = \frac{\sum(iX_i)}{\sum X_i} \quad (2)$$

where X_i is the abundance of the *n*-alkane with *i* number of carbon atoms.

4.4. δD Correction for the ice volume

We corrected δD values for global seawater isotopic changes caused by changes in continental ice volume using the simulated $\delta^{18}O_{\text{ice-volume}}$ data published in (Bintanja et al., 2005). The ice-volume correction for δD values is based on (Jouzel et al., 2003):

$$\delta D = \delta D_{\text{measured}} - 8\Delta\delta^{18}O_{\text{ice-volume}} \times \left(1 + \frac{\delta D_{\text{measured}}}{1000}\right) / \left(1 + 8\frac{\Delta\delta^{18}O_{\text{ice-volume}}}{1000}\right) \quad (3)$$

where $\delta^{18}O_{\text{ice-volume}}$ is the ice-volume contribution to changes in oceanic $\delta^{18}O$. The δD values discussed in this work are all referred to ice volume corrected values.

5. RESULTS

We measured four dominant long-chain odd-numbered *n*-alkanes from GIK 16160-3: *n*-C_{27}, *n*-C_{29}, *n*-C_{31} and *n*-C_{33}. Among them, *n*-C_{29} and *n*-C_{31} are the most abundant and *n*-C_{27} is the least abundant (Fig. 3a). Overall, the *n*-alkanes were more abundant during the Glacial (~15 ka and onward) and Deglacial (~15–10 ka) compared to the Holocene (~10 ka to present). This pattern likely reflects the closer proximity of the Zambezi River mouth and transport of reworked shelf sediments to the coring site during the last Glacial sea-level low stand as compared to the Holocene (Marz et al., 2008). The CPI ranges from 4.1 and 6.4 with an average CPI 5.5, suggesting that *n*-alkanes from the Zambezi catchment are typically derived from terrestrial plants. This is because the odd-over-even predominance of wax *n*-alkanes of terrestrial higher plants are characterized by CPI of >4 (Chikaraishi and Naraoka, 2004; Collister et al., 1994) whereas petroleum have CPI of ~1 (Collister et al., 1994). The ACL ranges between 29.4 and 30.5 throughout the core, further confirming that *n*-C_{29} and *n*-C_{31} are the dominant *n*-alkanes in the Zambezi catchment.

The magnitudes of δD fluctuation for each *n*-alkane homologue are distinctly different from each other (Fig. 3b). The ice-volume corrected δD values resulted in <5‰ depletion compared to the uncorrected raw values, with the overall patterns for all four *n*-alkanes unchanged (Fig. 3b and c). Among them, *n*-C_{33} has the largest variations, ranging between ~−175‰ and −140‰, whereas *n*-C_{29} only ranges from ~−150‰ to −135‰ from the Glacial to the early Holocene. In addition, the δD values of *n*-$C_{31, 33}$ are more depleted than those of *n*-$C_{27, 29}$ and the magnitude of δD differences among individual *n*-alkanes also vary throughout the record (Fig. 3c). For example, the most pronounced differences occurred during the last Glacial period with an average offset of 20‰ between *n*-C_{33} and *n*-C_{29}, whereas their offset is only 2‰ to 10‰ for the Holocene. δD trends of *n*-$C_{27,29}$ are very similar except between ~11 and 9 ka, which may be partially due to aquatic plants input to *n*-C_{27} (Ficken et al., 2000).

Similar patterns also apply to the $\delta^{13}C$ records of the four *n*-alkanes (Fig. 3d). For example, the $\delta^{13}C$ values of *n*-C_{33} are the most enriched, and record the largest magnitude of $\delta^{13}C$ variations, ranging from ~-29 to −22‰. In comparison, *n*-C_{29} is the most depleted, and varies from −32‰ to −27‰ (Fig. 3d). *n*-C_{27} and *n*-C_{31} have comparable $\delta^{13}C$ values, ranging from −32‰ to −25‰. Maximum offsets among the individual *n*-alkane $\delta^{13}C$ values (up to 6‰ between *n*-C_{33} and *n*-C_{29}) also occurred during the last Glacial period. The offsets decrease during the Deglacial and reach a minimum (1–2‰) during the Holocene (Fig. 3d), which are within the uncertainty of $\delta^{13}C$ values of individual homologues obtained from the modern plant studies (Rommerskirchen et al., 2006; Vogts et al., 2009). Overall, long-term trends in the offset between these four *n*-alkanes are remarkably similar in δD and $\delta^{13}C$ values (Fig. 3c and d).

6. DISCUSSION

6.1. Effect of vegetation types on $\delta^{13}C$ variability

The different ranges of $\delta^{13}C$ values for each *n*-alkane in our GIK 16160-3 record suggest that the proportional contributions of C_4 grasses and C_3 dicots varied between each homologue. The lighter $\delta^{13}C$ values in our record (Fig. 3) fall into the upper range of modern African woodland C_3 dicots that span from −37.7‰ to −29.1‰ for *n*-$C_{29,31}$ (Vogts et al., 2009). The heavier values correspond to a mixture of C_3 dicots and C_4 grasses as African C_4 grass *n*-$C_{29,31,33}$ range from −26.3‰ to −18.3‰ (Rommerskirchen et al., 2006). A gradual decrease in *n*-C_{33} values from ~−22 to −29‰ from the Glacial to the Holocene indicates that the catchment shifted from a dominant C_4 vegetation to a more evenly mix of C_3 dicots and C_4 grasses types. Similarly, the decrease of $\delta^{13}C_{n\text{-}C31,27}$ values from −25‰ to −32‰ also suggests that *n*-$C_{31,27}$ was mainly derived from C_4 plant types during the Glacial to a slightly mixed vegetation types during the Holocene. In comparison, the relative narrower $\delta^{13}C$ range from −27‰ to −32‰ for *n*-C_{29} implies it was less sensitive to C_3 and C_4 plant changes than the other homologues and that its contributions were dominated by C_3 plant types (Fig. 3d).

6.2. Controls on δD variability

The incoherent δD variations among individual homologues demonstrate that not all individual homologues can be straightforwardly interpreted as proxies for changes in rainfall because C_3 dicots and C_4 grasses affected individual δD_{alk} differently (Fig. 3c). Our $\delta^{13}C$ record suggests that C_4 grasses contributed a greater proportion to the two longer chain *n*-alkanes (*n*-$C_{31,33}$) than C_3 dicots. From Fig. 2 and the previous literature (i.e. Sachse et al., 2012) it is apparent that δD_{alk} of C_4 grasses are more depleted than that of C_3 dicots because the $\varepsilon_{alk\text{-}MAP}$ of C_4 grasses is significantly more depleted than that of C_3 dicots. The ~20‰ differences in δD values between *n*-C_{29} and *n*-C_{33} during the Glacial in our record can thus be explained by the distinctively different $\varepsilon_{alk\text{-}MAP}$ values (~30‰) for C_3 dicots and C_4 grasses (Fig. 2, Table 1). Therefore, changes in contributions from C_3 dicots and C_4 grasses were the primary cause for the different δD patterns of the four homologues in our record.

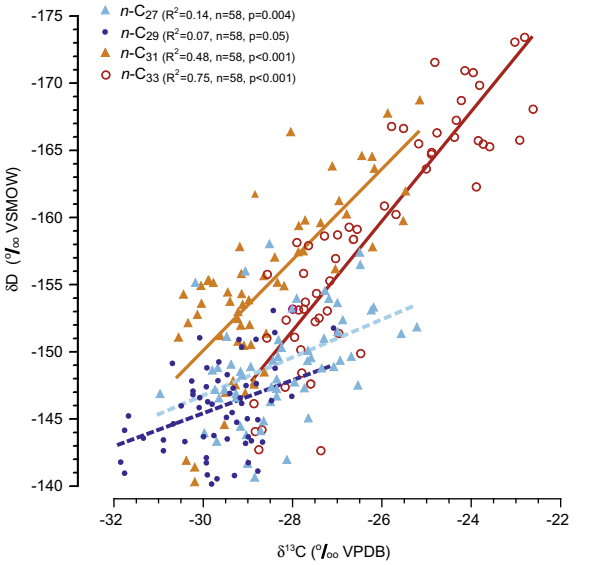

Fig. 4. Correlations between δD and $\delta^{13}C$ for four *n*-alkanes (*n*-$C_{33,31,29,27}$). The lack of correlation between δD and $\delta^{13}C$ for *n*-C_{29} and *n*-C_{27} suggest limited influence from C_4/C_3 vegetation type for these two homologues (dashed lines). In contrast, strong negative linear correlations between δD and $\delta^{13}C$ for *n*-C_{33} and *n*-C_{31} demonstrate that the increases in δD values were strongly influenced by the decreases in C_4 contributions over the Deglacial interval.

Furthermore, our data show that shifts in C_4 grasses and C_3 dicots have less effect on the short than long-chain *n*-alkanes. Strong negative linear correlations between δD and $\delta^{13}C$ values for *n*-C_{33} ($R^2 = 0.75$, $n = 58$, $p < 0.001$) and *n*-C_{31} ($R^2 = 0.48$, $n = 58$, $p < 0.001$) demonstrate that the increases in δD values were strongly influenced by the decreased contribution of C_4 grasses to these homologues, in particular during the Deglacial period (Fig. 4). In comparison the correlation between δD and $\delta^{13}C$ for *n*-C_{29} ($R^2 = 0.07$, $n = 58$, $p = 0.05$) and *n*-C_{27} ($R^2 = 0.14$, $n = 58$, $p < 0.01$) were much weaker, suggesting that δD values from these two homologues were less influenced by changes between C_4 grasses and C_3 dicots (Fig. 4). The combined δD and $\delta^{13}C$ records on multiple *n*-alkanes demonstrate that besides the influence of precipitation δD values changes in vegetation also played an essential role in affecting past changes in δD values of *n*-C_{31} and *n*-C_{33}. Monitoring changes in the relative importance of changes in precipitation and in plant functional types over time appears crucial to accurately interpret the δD_{alk} values to derive past changes in the hydrological cycle.

6.3. Mixing of *n*-alkanes in plant types

Stable isotope ratios of the longer chain lengths are more influenced by C_4 grass inputs than the shorter chain lengths because the longer chains *n*-C_{31} and *n*-C_{33} vs. the

shorter chains n-C_{29} and n-C_{27} display two distinct trends (Fig. 4). Such distinction is yet not entirely clear in modern plants because the n-C_{29} and n-C_{31} alkanes have generally been found in all plants (Sachse et al., 2012 and reference therein) and trees have wide range of chain lengths and overlap with grasses (i.e. Chikaraishi and Naraoka, 2003; Liu et al., 2006; Liu and Yang 2008). However, chemotaxonomic studies demonstrate that modern C_4 grasses from tropical Africa synthesize slightly more of the longer chain lengths such as C_{31} and C_{33}, resulting in ACL of ~30.7 (Rommerskirchen et al., 2006). In comparison, C_3 savanna trees and shrubs (dicots) synthesize a wider variation of chain lengths but are slightly more dominant with n-C_{29} and n-C_{31} and have an ACL of ~29.0 (Vogts et al., 2009). This evidence suggests that longer chain lengths are more susceptible to grass inputs than the shorter chain lengths for African vegetation types thus corroborating the conclusion drawn independently from our paleo δD and $\delta^{13}C$ results.

6.4. Vegetation corrections for δD of longer chain *n*-alkanes

Since n-C_{29} was the least influenced by changes of proportional contributions from C_4 grasses and C_3 dicots (Fig. 4), we used $\delta D_{n\text{-}C29}$ as the most robust indicator for precipitation. A recent study using δD_{alk} derived from 11 surface lake sediments in tropical Africa has also corroborated that $\delta D_{n\text{-}C29}$ is more robust than $\delta D_{n\text{-}C31}$ for reconstructing the isotopic composition of precipitation, as the latter may be derived from different plant functional types (Garcin et al., 2012). To evaluate the degree to which n-C_{33} and n-C_{31} were influenced by C_4 grasses relative to n-C_{29} we calculated the differences between n-C_{33} or n-C_{31} and n-C_{29} for $\delta^{13}C$ and δD. We found strong negative correlations between Δδ D and $\Delta\delta^{13}C$ for n-C_{33-29} ($R^2 = 0.85$, $n = 58$, $p < 0.001$) and for n-C_{31-29} ($R^2 = 0.70$, $n = 58$, $p < 0.001$) (Fig. 5), indicating that contrasting temporal changes recorded by δD of n-C_{33}, n-C_{31}, and n-C_{29} were primarily due to different C_3 tree vs. C_4 grass contributions to each n-alkane. We used the slope and intercept (Fig. 5) of the linear regression to account for the differences in C_3 tree vs. C_4 grass contributions on δD of n-C_{33} or n-C_{31} relative to n-C_{29} by applying the following equations:

$$\delta D_{\text{veg.corr.n}-C_{33}} = \delta D_{n-C_{33}} - [-3.4 \times (\delta^{13}C_{n-C_{33}} - \delta^{13}C_{n-C_{29}}) - 1.3] \quad (4)$$

$$\delta D_{\text{veg.corr.n}-C_{31}} = \delta D_{n-C_{31}} - [-3.2 \times (\delta^{13}C_{n-C_{31}} - \delta^{13}C_{n-C_{29}}) - 5.6] \quad (5)$$

where $\delta D_{n\text{-}C33}$ and $\delta D_{n\text{-}C31}$ are the measured values. Since the δD corrections for n-C_{33} or n-C_{31} are calculated relative to n-C_{29}, their trends approximate that of n-C_{29} (Fig. 6b). However, the vegetation corrected δD patterns of n-C_{33} or n-C_{31} homologues are more likely to accurately reflect rainfall δD values compared to the non-corrected values because our calculations demonstrate that the δD differences between n-C_{33} or n-C_{31} and n-C_{29} can be explained primarily by shifts from C_4 grasses to C_3 dicots (~85% and ~70%, respectively). As n-C_{27} is the least abundant homologues in our record and its δD values are not strongly affected by shifts in $\delta^{13}C$, we did not correct the vegetation effect on n-C_{27}.

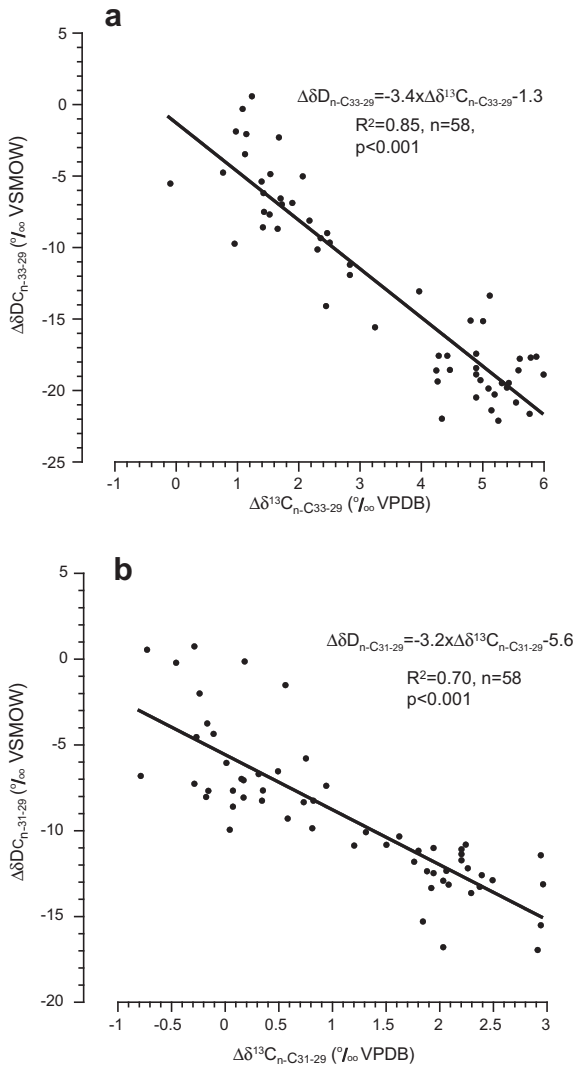

Fig. 5. Relationship between (a) $\Delta\delta D_{n\text{-}C33\text{-}29}$ and $\Delta\delta^{13}C_{n\text{-}C33\text{-}29}$; (b) $\Delta\delta D_{n\text{-}C31\text{-}29}$ and $\Delta\delta^{13}C_{n\text{-}C31\text{-}29}$, suggesting the proportional differences of C_4 and C_3 contribution affected the different patterns of δD and $\delta^{13}C$ of individual n-alkanes.

The fact that δD differences between n-alkanes for a large part can be explained by shifts between C_4 and C_3 vegetation type signifies that we can compare those differences to δD and $\delta^{13}C$ values of modern C_3 dicots and C_4 grasses. For our paleo data, the offsets between n-C_{33} and n-C_{29} are ~6‰ for $\delta^{13}C$ and ~20‰ for δD (Fig. 5). For n-alkanes derived from modern C_3 dicots and C_4 grasses, the offsets are ~12‰ for $\delta^{13}C$ and ~30‰ for δD (Fig. 2, Vogts et al., 2009; Chikaraishi and Naraoka, 2003). The offset for $\delta^{13}C$ in our record equates ~50% of that between modern C_3 dicot and C_4 grasses, and the offset for δD equates ~70%, demonstrating that the rate by which δD changes relative to $\delta^{13}C$ is fairly similar. The slightly greater change rate of δD relative to $\delta^{13}C$ in our record perhaps suggests that residual factors other than vegetation shifts also affected δD_{alk} in the Zambezi Catchment area. Evidence

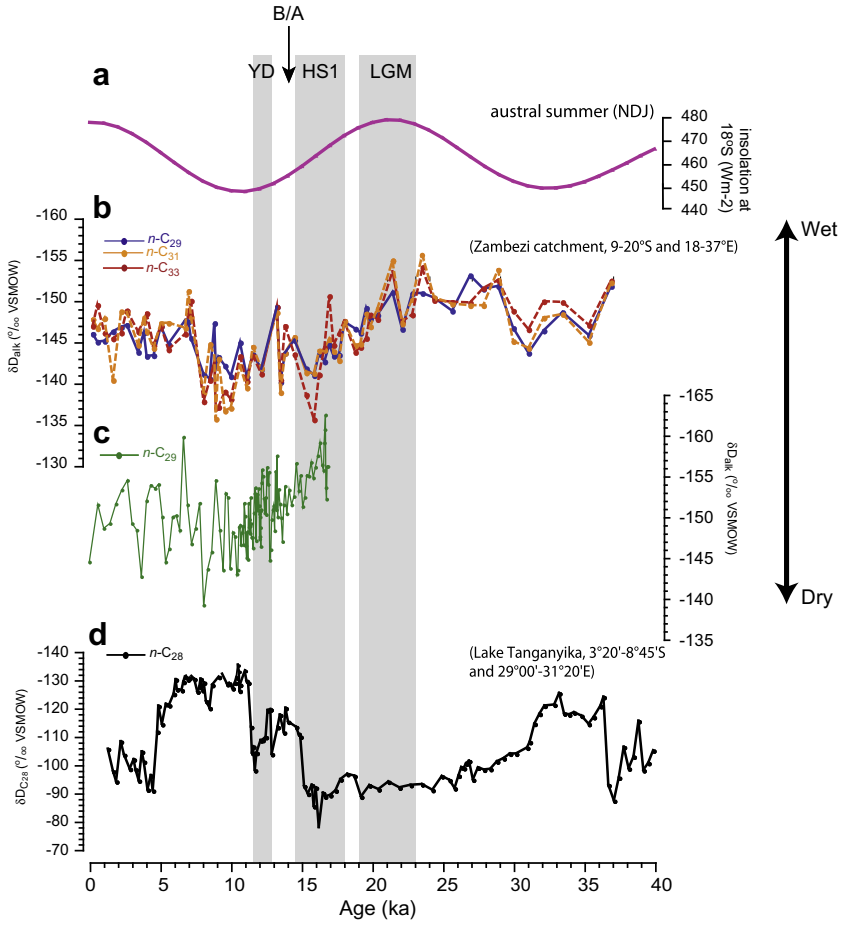

Fig. 6. (a) Austral summer (DJF) insolation at 18°S (Laskar et al., 2004); (b) $\delta D_{n\text{-}C29}$ (solid blue line) records are plotted with $\delta D_{n\text{-}C33}$ and $\delta D_{n\text{-}C31}$ (dashed line) after these two long chain *n*-alkanes factoring out the difference in contributions from C_4 grass and C_3 trees from Zambezi catchment (this study); (c) temporal variations in ice volume corrected $\delta D_{n\text{-}C29}$ (solid green line) from Schefuss et al. (2011); and (d) temporal variations in δD of *n*-acid from Lake Tanganyika (Tierney et al., 2008). Important climate events that were discussed in the text are marked either by grey bars or acronyms. These are: Holocene (~10–0 ka), YD, Younger Dryas Period (~13–10.5 ka); B/A, Bølling–Allerød (~14.6–13 ka); HS1, Heinrich Stadial 1 (~19–14.6 ka); LGM, Last Glacial Maximum (~23–19 ka); and MIS3, Marine Isotope Stage III (~60–23 ka).

indicates that the δD-enrichment due to soil-water evaporation (Hou et al., 2008) and leaf-water transpiration (Feakins and Sessions, 2010) affect δD_{alk} of woody plants. Generally, $\varepsilon_{alk\text{-}MAP}$ values are smaller in drier conditions/environment because there is more enrichment in plant water and more enrichment in precipitation due to lower precipitation amount (i.e Sachse et al., 2012 for the review). These climate-induced effects perhaps partially explain the large variability of $\varepsilon_{alk\text{-}MAP}$ within the C_3 dicots and C_4 grasses from the global perspective (Fig. 2 and Sachse et al., 2012). However, shift between C_4 and C_3 plant types explain more than 70% of δD variation in our core, suggesting evapotranspiration is less important than the effects linked to the physiology of C_3/C_4 vegetation types in tropical Africa as climate-induced factors eventually lead to the vegetation change adapted to these conditions. It is also possible that C_3 trees and C_4 grasses peak during different seasons, therefore utilizing different water sources with contrasting δD signatures. However, in a distinctly seasonal climate regime as in tropical southern Africa, plants take advantage of the seasonal water availability during the rainy season and hence produce the majority of their biomass during that season (Garcin et al., 2012). In addition, recent studies have demonstrated that leaf wax *n*-alkane from trees and grasses are synthesized early in the ontogeny of a leaf (Sachse et al., 2010; Kahmen et al., 2011). Hence it is plausible that most of the *n*-alkanes are synthesized using the same water source during the rainy season in austral summer in the Zambezi River catchment.

6.5. Paleohydrological implications

From a paleohydrological perspective, the δD values of $n\text{-}C_{29}$ infer substantial variations in monsoon rainfall throughout the last 37 kyr with values ranging from −155‰ to −135‰ (Fig. 6b). The depleted δD_{alk} values reflect high amounts of precipitation in low latitude (e.g. Niedermeyer et al., 2010; Schefuss et al., 2005, 2011; Konecky et al., 2011). Our rainfall record shows that tropical southern Africa experienced dry periods during the Deglacial and

the early Holocene (Fig. 6b). Wet phases are recorded for the late and mid-Holocene (~7 ka to present) and the late Marine Isotope Stage 3 (MIS3), the wettest period being recorded during the Last Glacial Maximum (LGM, ~23 to 19 ka).

The δD and $\delta^{13}C$ ranges prior to vegetation correction are broadly in agreement with long-term δD and $\delta^{13}C$ trends recorded in an adjacent record of δD_{alk} (ice volume corrected values) and $\delta^{13}C_{alk}$ from Zambezi River mouth covering the last 17 kyr only (Schefuss et al., 2011), but with our time resolution for the Deglacial interval being much lower. Schefuss et al. (2011) inferred enhanced rainfall during Younger Dryas (YD, ~12–10.5 ka) and Heinrich Stadial 1 period (HS1, ~19–14.6 ka) using $\delta D_{n\text{-}C31}$ rather than $\delta D_{n\text{-}C29}$. Since $\delta D_{n\text{-}C29}$ have a smaller range of magnitude than $\delta D_{n\text{-}C31}$ (Fig. 6c) we evaluated the effect of changing C_3/C_4 vegetation on δD from Schefuss et al. (2011) by correlating the $\delta^{13}C$ and δD values of $n\text{-}C_{29,31,33}$ (Supplementary Fig. 1). This analysis shows that changes in $\delta^{13}C$ values explains more than 50% of δD changes for $n\text{-}C_{33}$ ($R^2 = 0.53$, $n = 105$, $p < 0.001$) and 40% for $n\text{-}C_{31}$ ($R^2 = 0.40$, $n = 127$, $p < 0.001$), suggesting that the longer chain length $n\text{-}C_{33}$ or $n\text{-}C_{31}$ were likely to have been affected by shifts between C_3/C_4 vegetation changes whereas $n\text{-}C_{29}$ was the least affected ($R^2 = 0.13$, $n = 123$, $p < 0.001$) (Supplementary Fig. 1). The greater influence of vegetation shift on $n\text{-}C_{33}$ or $n\text{-}C_{31}$ than $n\text{-}C_{29}$ accords with the analysis from our core, suggesting that $n\text{-}C_{29}$ in the study by Schefuss et al. (2011) would reflect precipitation with a higher fidelity than $n\text{-}C_{31}$ and consequently dampen the δD magnitude but not affect the direction of precipitation trends. With $n\text{-}C_{29}$, HS1 would have experienced similar precipitation as the Holocene (Fig. 6c). That said, the C_3/C_4 vegetation correction is probably more critical when Glacial–interglacial timescales are considered tropical southern Africa. Nevertheless, accounting for vegetation changes may help reconciling differences observed in the magnitudes of the different *n*-alkanes homologues δD and $\delta^{13}C$ in the dataset of Schefuss et al. (2011).

The rainfall variability in the Zambezi catchment broadly corresponds to changes in summer insolation at 18°S during the last 37 kyr (Fig. 6a). Most strikingly, the LGM stands out as the wettest period of our record (Fig. 6b). The wet LGM contrasts with most records of precipitation from Eastern and southern Africa, and in particular with a record of δD of C_{28} *n*-acid from Lake Tanganyika (Tierney et al., 2008, Fig. 6d), north of the Zambezi catchment. The Tanganyika basin (3°20′–8°45′S and 29°00′–31°20′E) is situated on the boundary of woodland savannah and tropical rainforest (Fig. 1) and it has higher precipitation rate (1200 mm/yr) than the Zambezi catchment. Its precipitation is also controlled by the seasonal migrations of the Inter-tropical Convergence Zone (ITCZ) as well as moisture flux from the Indian Ocean and Congo air Boundary (Tierney et al., 2010). Overall, both δD records from the Zambezi catchment and from lake Tanganyika illustrate an anti-phasing in changes in the hydrological cycle (Fig. 6b and d). The apparent anti-phased precipitation trends recorded in East African lakes and our record support the notion of a meridional hinge zone mediated by ITCZ between equatorial and tropical southern Africa during the last glacial period (Tierney et al., 2010). Such pattern may be explained by a latitudinal asymmetry of precipitation rate and/or precipitation origin between these two catchments. It further supports that the ITCZ location during austral summer months was likely confined to 20°S during the LGM (Verschuren et al., 2009) because subtropical southern Africa was also dry during the LGM (Gasse et al., 2008 and reference therein).

For the Lake Tanganyika record, however, δD of $n\text{-}C_{28}$ acid was more enriched during the LGM than during the early Holocene by a magnitude of ~40‰, which is substantially larger than the change observed in our record. Yet, this 40‰ decrease recorded during the Deglacial is accompanied by a 10‰ decrease in $\delta^{13}C$ of $n\text{-}C_{28}$ (Tierney et al., 2010), suggesting that vegetation shifts occurred in response to rainfall changes in the lake Tanganyika catchment. The lack of information on the origin and isotopic values of different *n*-acid homologues in the record by Tierney et al. (2010) makes it challenging to assess how shifts in C_3/C_4 vegetation might have affected δD. Therefore, it appears crucial to have dual $\delta^{13}C$ and δD measurements from different *n*-acid or *n*-alkanes homologues in tropical sites in order to more accurately quantify the amplitude of past changes in rainfall.

7. CONCLUSION

Our work demonstrates that the δD_{alk} was not only controlled by changes in precipitation, but also by changes in photosynthetic pathways and plant functional types in southern tropical Africa in the past 37,000 years. The importance of these biological effects on δD is supported by the significant differences in ε_{alkMAP} between C_4 grasses and C_3 dicots from literature compilation data. Importantly, for areas where vegetation is composed of a mixture of C_4 grasses and C_3 dicots, dual measurements of δD and $\delta^{13}C$ on multiple *n*-alkanes are essential for disentangling the vegetation effect from the hydrological effects on *n*-alkane δD temporal shifts. After accounting for different C_3/C_4 vegetation contributions to each *n*-alkanes, the differences in δD of all individual homologues show similar trends and may provide similar information on past changes in the regional hydrological cycle. This reinforces the idea that leaf wax δD provide realistic, robust and reliable tools for reconstructing past changes in the low latitudes hydrological cycle.

ACKNOWLEDGMENTS

The authors thank the captain, the crew and the participants of Meteor cruise 75/3 for obtaining core GIK 16160-3. This project was funded by the German Science Foundation (DFG) and DFG ExCl 80 "the Future Ocean". T.L. was also supported by Carlsbergfondet and JCI-2009-04933. We thank R. Tjallingii for XRF core scanning, and S. Koch and C. Rautenstrauch for laboratory assistances. We also thank P.M. Grootes, M. Nadeau, and staff of Leibniz-Labor at CAU for ^{14}C-AMS dating. Finally we thank two anonymous reviewers and Dr. F. McInerney for their valuable and constructive comments that improved this manuscript.

APPENDIX A. SUPPLEMENTARY DATA

Supplementary data associated with this article can be found, in the online version, at http://dx.doi.org/10.1016/j.gca.2012.10.016.

REFERENCE

Bi X. H., Sheng G. Y., Liu X. H., Li C. and Fu J. M. (2005) Molecular and carbon and hydrogen isotopic composition of n-alkanes in plant leaf waxes. *Org. Geochem.* **36**, 1405–1417.

Bintanja R., van de Wal R. S. W. and Oerlemans J. (2005) Modelled atmospheric temperatures and global sea levels over the past million years. *Nature* **437**, 125–128.

Bowen G. J. (2010) Isoscapes: spatial pattern in isotopic biogeochemistry. *Annu. Rev. Earth Planet. Sci.* **38**, 161–187.

Bowen G. J., Ehleringer J. R., Chesson L. A., Thompson A. H., Podlesak D. W. and Cerling T. E. (2009) Dietary and physiological controls on the hydrogen and oxygen isotope ratios of hair from mid-20th century indigenous populations. *Am. J. Phys. Anthropol.* **139**, 494–504.

Bowen G. J. and Revenaugh J. (2003) Interpolating the isotopic composition of modern meteoric precipitation. *Water Resour. Res.* **39**, 13.

Cerling T. E., Harris J. M., MacFadden B. J., Leakey M. G., Quade J., Eisenmann V. and Ehleringer J. R. (1997) Global vegetation change through the Miocene/Pliocene boundary. *Nature* **389**, 153–158.

Chikaraishi Y. and Naraoka H. (2003) Compound-specific delta D-delta C-13 analyses of n-alkanes extracted from terrestrial and aquatic plants. *Phytochemistry* **63**, 361–371.

Chikaraishi Y. and Naraoka H. (2004) Carbon and hydrogen isotopic compositions of sterols in riverine-marine sediments. *Geochim. Cosmochim. Acta* **68**, A338.

Collins J. A., Schefuss E., Heslop D., Mulitza S., Prange M., Zabel M., Tjallingii R., Dokken T. M., Huang E. Q., Mackensen A., Schulz M., Tian J., Zarriess M. and Wefer G. (2011) Interhemispheric symmetry of the tropical African rainbelt over the past 23,000 years. *Nat. Geosci.* **4**, 42–45.

Collister J. W., Rieley G., Stern B., Eglinton G. and Fry B. (1994) Compound-specific delta-C-13 analyses of leaf lipids from plants with differing carbon-dioxide metabolisms. *Org. Geochem.* **21**, 619–627.

Feakins S. J. and Sessions A. L. (2010) Controls on the D/H ratios of plant leaf waxes in an arid ecosystem. *Geochim. Cosmochim. Acta* **74**, 2128–2141.

Ficken K. J., Li B., Swain D. L. and Eglinton G. (2000) An n-alkane proxy for the sedimentary input of submerged/floating freshwater aquatic macrophytes. *Org. Geochem.* **31**, 745–749.

Garcin Y., Schwab V. F., Gleixner G., Kahmen A., Todou G., Sene O., Onana J.-M., Achoundong G. and Sachse D. (2012) Hydrogen isotope ratios of lacustrine sedimentary n-alkanes as proxies of tropical African hydrology: insights from a calibration transect across Cameroon. *Geochim. Cosmochim. Acta* **79**, 106–126.

Gasse F., Chalie F., Vincens A., Williams M. A. J. and Williamson D. (2008) Climatic patterns in equatorial and southern Africa from 30,000 to 10,000 years ago reconstructed from terrestrial and near shore proxy data. *Quat. Sci. Rev.* **27**, 2316–2340.

Gimeno L., Drumond A., Nieto R., Trigo R. M. and Stohl A. (2010) On the origin of continental precipitation. *Geophys. Res. Lett.*, 37.

Goddard L. and Graham N. E. (1999) Importance of the Indian Ocean for simulating rainfall anomalies over eastern and southern Africa. *J. Geophys. Res. Atmos.* **104**, 19099–19116.

Hou J., D'Andrea W. J., MacDonald D. and Huang Y. (2007) Evidence for water use efficiency as an important factor in determining the delta D values of tree leaf waxes. *Org. Geochem.* **38**, 1251–1255.

Hou J. Z., D'Andrea W. J. and Huang Y. S. (2008) Can sedimentary leaf waxes record D/H ratios of continental precipitation? Field, model, and experimental assessments. *Geochim. Cosmochim. Acta* **72**, 3503–3517.

Hou J. Z., D'Andrea W. J., MacDonald D. and Huang Y. S. (2007) Hydrogen isotopic variability in leaf waxes among terrestrial and aquatic plants around Blood Pond, Massachusetts (USA). *Org. Geochem.* **38**, 977–984.

Huang Y., Street-Perrott F. A., Metcalfe S. E., Brenner M., Moreland M. and Freeman K. H. (2001) Climate change as the dominant control on glacial–interglacial variations in C-3 and C-4 plant abundance. *Science* **293**, 1647–1651.

Huang Y. S., Dupont L., Sarnthein M., Hayes J. M. and Eglinton G. (2000) Mapping of C-4 plant input from North West Africa into North East Atlantic sediments. *Geochim. Cosmochim. Acta* **64**, 3505–3513.

Jouzel J., Vimeux F., Caillon N., Delaygue G., Hoffmann G., Masson-Delmotte V. and Parrenin F. (2003) Magnitude of isotope/temperature scaling for interpretation of central Antarctic ice cores. *J. Geophys. Res. Atmos.* **108**. http://dx.doi.org/10.1029/2002jd002677.

Kahmen A., Dawson T. E., Vieth A. and Sachse D. (2011) Leaf wax n-alkane δD values are determined by early in the ontogeny of *Populus trichocarpa* leaves when grown under controlled environmental conditions. *Plant, Cell Environ.* **34**, 1639–1651.

Konecky B., Russell J. M., Johnson T. C., Brown E. T., Berke M. A., Werne J. P. and Huang Y. (2011) Atmospheric circulation patterns during late Pleistocene climate changes at Lake Malawi, Africa. *Earth Planet. Sci. Lett.* **312**, 318–326.

Krull E., Sachse D., Mugler I., Thiele A. and Gleixner G. (2006) Compound-specific delta(13)C and delta(2)H analyses of plant and soil organic matter: a preliminary assessment of the effects of vegetation change on ecosystem hydrology. *Soil Biol. Biochem.* **38**, 3211–3221.

Laskar J., Robutel P., Joutel F., Gastineau M., Correia A. C. M. and Levrard B. (2004) A long-term numerical solution for the insolation quantities of the Earth. *Astron. Astrophys.* **428**, 261–285.

Liu W. G. and Huang Y. S. (2005) Compound specific D/H ratios and molecular distributions of higher plant leaf waxes as novel paleo environmental indicators in the Chinese Loess Plateau. *Org. Geochem.* **36**, 851–860.

Liu W. G. and Yang H. (2008) Multiple controls for the variability of hydrogen isotopic compositions in higher plant n-alkanes from modern ecosystems. *Glob. Change Biol.* **14**, 2166–2177.

Liu W. G., Yang H. and Li L. W. (2006) Hydrogen isotopic compositions of n-alkanes from terrestrial plants correlate with their ecological life forms. *Oecologia* **150**, 330–338.

Livingstone D. A. and Clayton W. D. (1980) An attitudinal cline in tropical African grass flora and its paleoecological significance. *Quat. Res.* **13**, 392–402.

Marz C., Hoffmann J., Bleil U., De Lange G. J. and Kasten S. (2008) Diagenetic changes of magnetic and geochemical signals by anaerobic methane oxidation in sediments of the Zambezi deep-sea fan (SW Indian Ocean). *Mar. Geol.* **255**, 118–130.

Marzi R., Torkelson B. E. and Olson R. K. (1993) A revised carbon preference index. *Org. Geochem.* **20**, 1303–1306.

McInerney F. A., Helliker B. R. and Freeman K. H. (2011) Hydrogen isotope ratios of leaf wax n-alkanes in grasses are insensitive to transpiration. *Geochim. Cosmochim. Acta* **75**, 541–554.

Moore A. E., Coterill F. P. D., Main M. P. L. and Williams H. B. (2007) The Zambezi river. In *Large Rivers: Geomorphology and Management* (ed. A. Gupta). John Wiley & Sons, Ltd., pp. 311–333.

Nicholson S. E. (2000) The nature of rainfall variability over Africa on time scales of decades to millenia. *Global Planet. Change* **26**, 137–158.

Niedermeyer E. M., Schefuss E., Sessions A. L., Mulitza S., Mollenhauer G., Schulz M. and Wefer G. (2010) Orbital- and millennial-scale changes in the hydrologic cycle and vegetation in the western African Sahel: insights from individual plant wax δD and $\delta^{13}C$. *Quat. Sci. Rev.* http://dx.doi.org/10.1016/j.quascirev.2010.06.039.

Pedentchouk N., Sumner W., Tipple B. and Pagani M. (2008) Delta (13)C and delta D compositions of n-alkanes from modern angiosperms and conifers: an experimental set up in central Washington State, USA. *Org. Geochem.* **39**, 1066–1071.

Polissar P. J. and Freeman K. H. (2010) Effects of aridity and vegetation on plant-wax delta D in modern lake sediments. *Geochim. Cosmochim. Acta* **74**, 5785–5797.

R-Development-Core-Team (2010) *R: A Language and Environment for Statistical Computing*. R Foundation for Statistical Computing, Vienna, Austria.

Reimer P. J., Baillie M. G. L., Bard E., Bayliss A., Beck J. W., Blackwell P. G., Ramsey C. B., Buck C. E., Burr G. S., Edwards R. L., Friedrich M., Grootes P. M., Guilderson T. P., Hajdas I., Heaton T. J., Hogg A. G., Hughen K. A., Kaiser K. F., Kromer B., McCormac F. G., Manning S. W., Reimer R. W., Richards D. A., Southon J. R., Talamo S., Turney C. S. M., van der Plicht J. and Weyhenmeye C. E. (2009) Intcal09 and Marine09 radiocarbon age calibration curves, 0–50,000 years Cal Bp. *Radiocarbon* **51**, 1111–1150.

Rommerskirchen F., Plader A., Eglinton G., Chikaraishi Y. and Rullkotter J. (2006) Chemotaxonomic significance of distribution and stable carbon isotopic composition of long-chain alkanes and alkan-1-ols in C-4 grass waxes. *Org. Geochem.* **37**, 1303–1332.

Sachse D., Billault I., Bowen G. J., Chikaraishi Y., Freeman K. H., Magill C. R., McInerney F. A., van der Meer M. T. J., Polissar P., Ribons R. J., Sachs J. P., Schmidt H.-L., Sessions A. L., White J. W., West J. B. and Kahmen A. (2012) Molecular paleohydrology: interpreting the hydrogen-isotopic composition of lipid biomarkers from photosynthesizing organisms. *Annu. Rev. Earth Planet. Sci.* **40**, 221–249.

Sachse D., Kahmen A. and Gleixner G. (2009) Significant seasonal variation in the hydrogen isotopic composition of leaf-wax lipids for two deciduous tree ecosystems (*Fagus sylvativa* and *Acer pseudoplatanus*). *Org. Geochem.* **40**, 732–742.

Sachse D., Radke J. and Gleixner G. (2004) Hydrogen isotope ratios of recent lacustrine sedimentary n-alkanes record modern climate variability. *Geochim. Cosmochim. Acta* **68**, 4877–4889.

Sachse D., Radke J. and Gleixner G. (2006) Delta D values of individual n-alkanes from terrestrial plants along a climatic gradient – Implications for the sedimentary biomarker record. *Org. Geochem.* **37**, 469–483.

Sachse D., Gleixner G., Wilkes H. and Kahmen A. (2010) Leaf wax n-alkane δD values of field-grown barley reflect leaf water δD values at the time of leaf formation. *Geochim. Cosmochim. Acta* **74**, 6741–6750.

Schefuss E., Kuhlmann H., Mollenhauer G., Prange M. and Patzold J. (2011) Forcing of wet phases in southeast Africa over the past 17,000 years. *Nature* **480**, 509–512.

Schefuss E., Schouten S. and Schneider R. R. (2005) Climatic controls on central African hydrology during the past 20,000 years. *Nature* **437**, 1003–1006.

Sessions A. L., Burgoyne T., Schimmelmann A. and Hayes J. M. (1999) Fractionation of hydrogen isotopes in lipid biosynthesis. *Org. Geochem.* **30**, 1193–1200.

Sessions A. L. (2006) Seasonal changes in D/H fractionation accompanying lipid biosynthesis in *Spartina alterniflor*. *Geochim. Cosmochim. Acta* **70**, 2153–2162.

Smith F. A. and Freeman K. H. (2006) Influence of physiology and climate on delta D of leaf wax n-alkanes from C-3 and C-4 grasses. *Geochim. Cosmochim. Acta* **70**, 1172–1187.

Still C. J., Berry J. A., Collatz G. J. and DeFries R. S. (2003) Global distribution of C-3 and C-4 vegetation: Carbon cycle implications. *Glob. Biogeochem. Cycles* **17**. http://dx.doi.org/10.1029/2001GB001807.

Stuiver M. and Reimer P. J. (1993) Extended C-14 data-base and revised Calib 3.0 C-14 age calibration program. *Radiocarbon* **35**, 215–230.

Tierney J. E., Russell J. M. and Huang Y. S. (2010) A molecular perspective on Late Quaternary climate and vegetation change in the Lake Tanganyika basin, East Africa. *Quat. Sci. Rev.* **29**, 787–800.

Tierney J. E., Russell J. M., Huang Y. S., Damste J. S. S., Hopmans E. C. and Cohen A. S. (2008) Northern hemisphere controls on tropical southeast African climate during the past 60,000 years. *Science* **322**, 252–255.

Timberlake J. (2000) Biodiversity of the Zambezi Basin. In *Occasional Publications in Biodiversity*. Biodiversity Foundation for Africa, Bulawayo.

Verschuren D., Damste J. S. S., Moernaut J., Kristen I., Blaauw M., Fagot M., Haug G. H and Challacea Project Members (2009) Half-precessional dynamics of monsoon rainfall near the East African Equator. *Nature* **462**, 637–641.

Vogts A., Moossen H., Rommerskirchen F. and Rullkotter J. (2009) Distribution patterns and stable carbon isotopic composition of alkanes and alkan-1-ols from plant waxes of African rain forest and savanna C-3 species. *Org. Geochem.* **40**, 1037–1054.

Walford H. L., White N. J. and Sydow J. C. (2005) Solid sediment load history of the Zambezi Delta. *Earth Planet. Sci. Lett.* **238**, 49–63.

Yang H. and Huang Y. S. (2003) Preservation of lipid hydrogen isotope ratios in Miocene lacustrine sediments and plant fossils at Clarkia, northern Idaho, USA. *Org. Geochem.* **34**, 413–423.

Associate Editor: Miryam Bar-Matthews